General Disclaimer

One or more of the Following Statements may affect this Document

- This document has been reproduced from the best copy furnished by the organizational source. It is being released in the interest of making available as much information as possible.

- This document may contain data, which exceeds the sheet parameters. It was furnished in this condition by the organizational source and is the best copy available.

- This document may contain tone-on-tone or color graphs, charts and/or pictures, which have been reproduced in black and white.

- This document is paginated as submitted by the original source.

- Portions of this document are not fully legible due to the historical nature of some of the material. However, it is the best reproduction available from the original submission.

R/W Pilot J. Kaufman, 735

Second Quarterly Report

for

DEVELOPMENT OF UNIFORM AND PREDICTABLE BATTERY MATERIALS FOR NICKEL CADMIUM AEROSPACE CELLS

Covering Period
August 8 through November 7, 1968

Contract No. NAS5-11561

Prepared by
Tyco Laboratories, Inc.
Waltham, Massachusetts 02154

for
National Aeronautics and Space Administration
Goddard Space Flight Center
Greenbelt, Maryland

Second Quarterly Report

for

DEVELOPMENT OF UNIFORM AND PREDICTABLE BATTERY MATERIALS FOR NICKEL CADMIUM AEROSAPCE CELLS

by

Helen Feng
Robert A. Cattabriga
George F. Hurley
John M. Parry

Covering Period
August 8 through November 7, 1968

Contract No. NAS5-11561

Goddard Space Flight Center

Contracting Officer
A. L. Essex

Technical Monitor
Gerald Halpert

Prepared by

Tyco Laboratories, Inc.
Waltham, Massachusetts 02154

Project Manager
John M. Parry

for

National Aeronautics and Space Administration
Goddard Space Flight Center
Greenbelt, Maryland

ABSTRACT

This report describes the initial experiments carried out on the sintering of carbonyl nickel powders for the fabrication of porous nickel plaque for nickel cadmium battery plates. Emphasis was placed on loose sintering of the powders without a support screen to facilitate a detailed study of the sintering characteristics of the powder. The initial experiments involved the establishment of a flat temperature profile in the sintering zone of the furnace and optimization of mold design in order to form highly uniform plaques. The results presented here relate to the effect of sintering time and sintering temperature on plaque characteristics. The plaques were characterized in terms of porosity, thickness, surface area, pore size distribution, electrical conductivity and mechanical strength. Detailed metallographic analysis was carried out on selected plaques.

The porosity and thickness were found to be relatively insensitive to the sintering time and temperature. For example, plaques prepared at 800 and 900° C showed porosities of 86 and 84% respectively for thicknesses of 0.021 and 0.022 inches. The electrical resistivity, however, fell from 4.47×10^{-4} ohm cm to 2.70×10^{-4} ohm cm. The results for the mean pore diameter obtained metallographically (19.6 μ) and by mercury porosimetry (7.8 μ) were not in good agreement. Possible reasons for this discrepancy are discussed.

CONTENTS

I. INTRODUCTION

This project seeks to specify the conditions under which reproducible and uniform nickel cadmium battery plates can be prepared and to identify uniform plates in nondestructive tests.

In the first report on this program we have reviewed the literature on nickel cadmium battery plate fabrication and examined the present practices in industrial production. The principal points made were (a) that uniformity in the physical characteristics of each macroscopic area of each plate is essential for reproducibility and predictability in performance and (b) that in general, the attention paid to quality control and quality assurance in battery plate manufacture is not adequate for materials intended for aerospace application. The first report also included an analysis of the variability from batch to batch of the physical properties of INCO carbonyl nickel powders. These are the only powders used in battery plaque fabrication in the United States.

During this report period the objectives were to study the sintering behavior of these powders and to examine variations in the sintered plaque characteristics as a function of the sintering variables and the physical characteristics of the powder. Our initial investigations were based on a loose or gravity sintering technique in a controlled atmosphere furnace with a very flat temperature profile. This was chosen for the first approach because of the relative simplicity of the operation and because in the absence of the support screen (essential in other manufacturing methods), it affords more straightforward observation of the sintering behavior of the nickel powders. The principal alternative method, that of slurry coating of a nickel screen, offers advantages in plaque intended for battery plate use and will be used routinely when we have established the sintering characteristics of the powders.

This report describes our experiences with the loose sintering technique, particularly in problems of mold design. Measurements of porosity, pore size distribution, surface area, and electrical resistivity are presented, along with the results of quantitative metallographic analysis.

II. PLAQUE PRODUCTION BY LOOSE SINTERING

The first approach to the experimental study of plaque production has been the loose or gravity sintering of nickel powders. Since the incorporation of a supporting grid or screen tends to obscure the effects of processing changes, these first experiments were made without a support.

A. Temporary Sintering Furnace

Late delivery of the hydrogen furnace designed for this project necessitated starting the work in a smaller furnace. This furnace, built by the American Electric Furnace Company, used 12 glow bars for heating and has a maximum temperature of about 1500°C. The control system used a bucking current which is switched on and off by the controller to hold the temperature at a preset level. Because this system was originally designed for much higher temperature operation, the control was ineffective in the range of temperatures in which we were working. Our only means of temperature control was therefore the current settings on the Variac with the controller switched off. This means of control was adequate but resulted in lengthy periods to change the desired temperature.

Furthermore, the mullite muffle had to be changed for one of Inconel. This was necessary since a cold work load cannot be suddenly inserted into a hot mullite muffle without cracking it. The metallic muffle is also desirable with a hydrogen atmosphere from the standpoint of safety.

The back end of the muffle was sealed by welding an Inconel plate over it; the atmosphere gas entered through a tube welded to the back plate. The working end of the muffle was secured with a loosely fitting porous fire brick, slotted to fit around thermocouples and a support rod for the work piece. The muffle was flushed with argon before admitting hydrogen. The hydrogen was purified by passing through a catalytic oxygen remover and dried by a molecular sieve. It was burned off at the working end of the muffle.

A flat central temperature zone was obtained in the muffle with a $\pm$ 3°C temperature variation over 6 inches. This level profile could be maintained over a temperature range between 600 and 800°C.

B. New Sintering Furnace

This furnace (Fig. 1), designed for this project, was installed in late September. It is also a batch type unit designed for use at temperatures between 600 and 1100°C with a hydrogen atmosphere.

The heating system consists of wire wound heaters arranged in three zones. The relative power to each zone is limited by separate trimpots. Temperature in the central zone is sensed by a thermocouple. The output of the thermocouple drives a current proportioning temperature control system. As the temperature in the center of the furnace approaches the set temperature, power to all three zones is reduced. In practice, the temperature inside the muffle remains stable, a few degrees below the set temperature. The temperature does not oscillate about the set point as it would with the on-off type of control system.

The temperature profile within the muffle was leveled by the same technique described above. The final adjustments gave a 13 inch flat profile with a $\pm$ 2°C deviation at 850°C. It was discovered that the temperature profile was quite sensitive to the temperature of the water jacket at the muffle entrance. Particular attention was given to maintaining a constant temperature in the water jacket by controlling the water flow rate.

The gas flow system is designed to provide a working atmosphere of hydrogen, although any other inert atmosphere may be used. Nitrogen is run through the muffle at a rate of 20 CFH during idling to protect the Inconel muffle from oxidation. At the beginning of a sintering run, the specimen tray is placed in the cooled end of the muffle. The hydrogen start switch is then turned on. After 5 minutes of flushing with nitrogen, the hydrogen valve is opened. The hydrogen is burned at the muffle entrance by a flame curtain, shown in Fig. 1. Failure of N_2 or H_2 gas pressure, electric power, or the flame curtain will sound an alarm, and shut off the hydrogen.

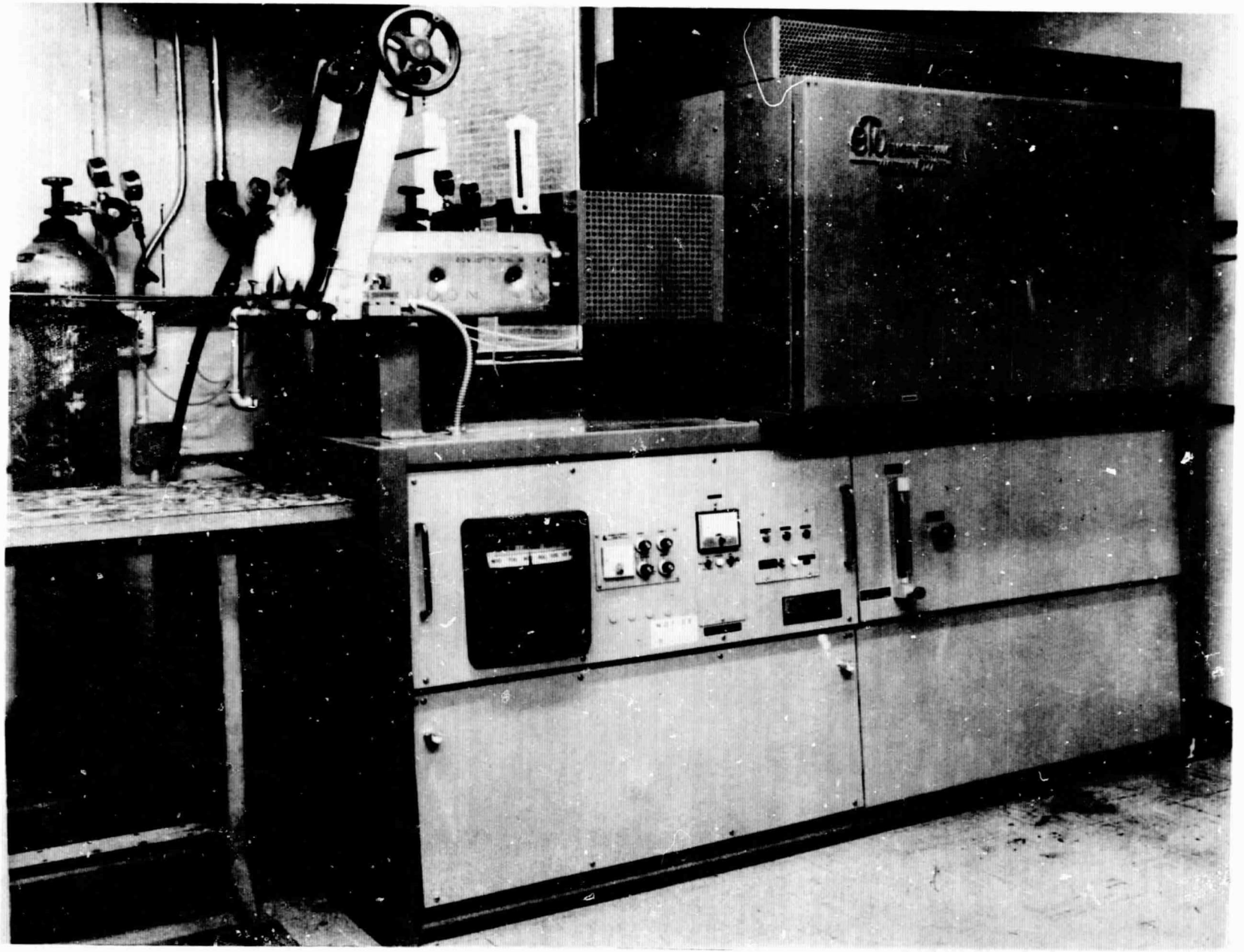

Fig. 1 Sintering furnace.

C. Molds and Filling Techniques

The mold used to contain the powders during sintering has evolved through several forms. The first mold, used only in the small furnace, was a 3/8 inch stainless steel plate with a 1 x 3 x 0.030 inch undercut. We found that more than 20 minutes were required to reach peak temperature, because of poor thermal contact with the circular muffle and the extremely high thermal mass of the plate.

New molds were prepared using 1/8 inch stainless steel with a 4 x 6 x 0.030 inch undercut. This mold, too, required a heat up period, but this was shortened to 5-10 minutes and reached 90% of peak temperature very quickly. The mold is manipulated in the furnace by means of a long rod attached with a yoke.

This mold gave rise to new problems. At temperatures greater than 800°, the sample tended to adhere to the plate. ZrO_2 powder effectively prevented adhesion but was also trapped in the bottom surface of the sintered plaque. In addition, removal of the mold into the cold section of the muffle resulted in warping.

In an attempt to eliminate both problems, we have switched to graphite molds, 3/16 inches thick. These molds do not warp and require only an extremely thin layer of ZrO_2 to prevent adhesion. The graphite mold also heats up more quickly, in about 5 minutes.

The filling techniques have been the same for all molds. Nickel powder is sieved directly into the undercut, the sieving being used to ensure a more uniform loose density. The top surface is smoothed and the excess powder removed by scraping with a steel straight edge.

III. PLAQUE CHARACTERIZATION

To date, characterization has been carried out with the object of perfecting sintering techniques and determining the general effects of process variables on the physical characteristics of loose sintered plaques. These results are presented in Table I. Studies have been carried out to determine average density, surface area, porosity, pore size distribution and electrical conductivity. An apparatus was built to determine mechanical strength in four-point bending.

A. Plaque Density and Metallography

The sintered density of all plaques was determined from the weight and dimensions. In the cases of plaques with irregular shrinkage, the area of the flat is determined by tracing on graph paper, then comparing the weight of the traced paper and a standard area weight.

Samples from sintered plaques were prepared for metallographic examination by impregnating the pore space with an epoxy resin. The epoxy, by filling all pores, prevents distortion of the structure during polishing. After impregnation, the samples were mounted in bakelite and sectioned. Sections perpendicular to the plane of the plaque were prepared for viewing by standard polishing techniques with silicon carbide papers and a 1 μ diamond polishing wheel. Samples were viewed and photographed without etching, since etching tended to obscure the otherwise sharp boundaries of the nickel skeleton. Magnification was accurately determined by means of a stage micrometer in order to be able to measure a mean pore size (mean free path).

Figure 2 is a typical micrograph of the sintered structure of a plaque. Note that only particles having a sharp boundary are considered to be in the plane of the photograph. Others below the surface of the epoxy are not considered in the quantitative analysis. The area fraction of the nickel may be determined in several ways as has been described by Smith and Guttman.*

* C. S. Smith and L. Guttman, Trans. AIME 197, 81 (1953).

TABLE I

Sintering Conditions for Plaques LNI → LN 25

Plaque No. LN	Powder Type	Sintering Time min	Sintering Temp. °C	Porosity %	Plaque No. LN	Powder Type	Sintering Time min	Sintering Temp. °C	Porosity %
1	255	30	820	86	14	255	30	900	83.5
2	255	20	822	87	15	287	30	900	81
3	255	10	817	89	16	255	30	800	87
4	255	5	805	80	17	287	30	800	83
5	255	30	728	90	18	255	15	800	88
6	255	20	720	90	19	255	60	800	87.5
7	255	10	700	88	20	287	15	800	84
8	255	5	673	90	21	287	60	800	83.5
9	255	39	609	88.5	22	255	15	900	87.5
10	255	Not sintered - slurry coating experiments			23	255	60	900	84.5
11	255				24	287	15	900	84.5
12	287	30	810	87	25	287	60	900	81.5
13	255	30	803	86					

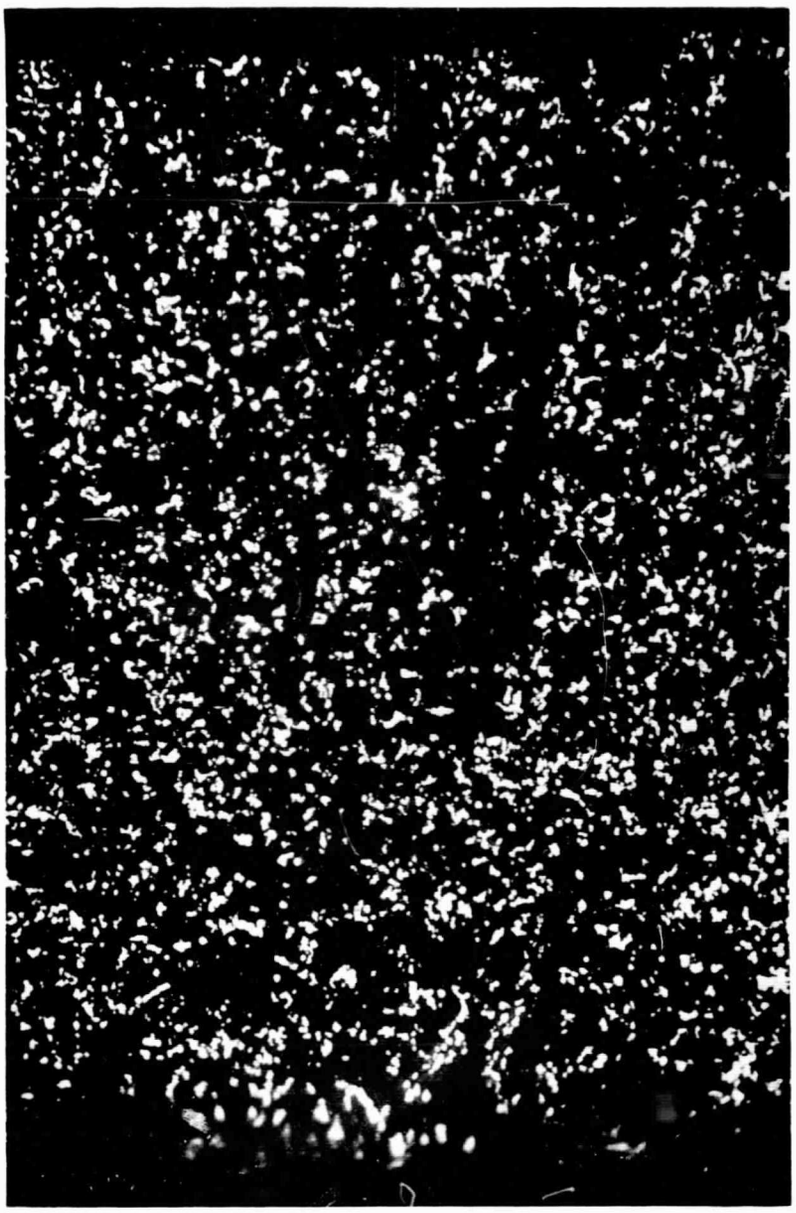

Fig. 2 Metallograph of a section of LN-3 (epoxy impregnated). 196X

The first method we tried was to place a 0.1" grid on a transparent backing over the micrograph and to count the number of grid intersections lying on the solid phase. The percent porosity P is then defined by

$$P = 100 - \frac{\text{number of intersections in the solid phase}}{\text{total number of intersections}} \times 100$$

This method has the advantages of high accuracy if a sufficiently large incremental area is counted. However, the method becomes critically sensitive to very localized deviations from average parameters if too small an area is considered. The laboriousness of counting even 10 percent of the area of a photograph makes this impractical in our case.

A second method was adopted to shorten the time required for analysis. This is the method of measuring intercept lengths along straight lines laid randomly over the section. The accuracy of this technique was established by reckoning the area fraction of pore phase after each line was counted and continuing to add lines until the average value did not change.

Volume fraction pores (% porosity) and pore mean free path may be calculated from a single measurement as follows. The volume fraction pores is simply

$$\frac{\Sigma L_m}{\Sigma L} = \frac{\text{length of lines in pore phase}}{\text{total length of lines}} = \text{volume fraction porosity}$$

Also

$$\frac{2\,\Sigma L_m}{\text{magnification} \times \text{number of intersections}} = \lambda_m = \text{mean free path in pores. (average pore dia.)}$$

The measurements completed to date are presented in Table II.

TABLE II

Quantitative Metallography

Plaque No.	Powder Type	Sintering Conditions Time (min)	Temp. °C	Average Porosity %	Metallographic Porosity %	Average Pore dia. (μ)
LN1	255	30	820	86	85.9	19.2
LN2	255	20	822	87	72.3	17.3
LN3	255	10	817	89	86.5	22.0
LN4	255	5	805	80	88.4	19.6
LN5	255	30	728	90	87.0	18.3
LN6	255	20	720	90	79.6	21.2
LN7	255	10	700	88	89.0	22.5
LN8	255	5	673	90	86.0	22.1

There have been few surprises in these exploratory experiments. Of key interest are the results for LN-1 to LN-5 showing that in the range of temperatures from 675 to 800°C, neither time nor temperature has a significant effect on density or pore phase mean free path. For the first series, for example, the furnace temperature was held at 800°C, for a range of sintering times between 5 and 30 minutes. Average density increased only 2 to 3 percent at the longer times. Further, the irregular changes in density between, say, 5 and 10 minutes at temperature suggest that variability is more strongly influenced by the way in which powder is put down in the mold rather than by the sintering parameters.

The density (percent porosity) measured metallographically differed in all cases from the average density by amounts up to 14 percent, providing a further indication that mold filling rather than sintering controls the nature and uniformity of the product. This difficulty will be circumvented in slurry coating methods of plaque manufacture.

Generally, the pore phase mean free path, λ_m, was an inverse function of the density. However, in the case of LN4, for which two micrographs were examined, this relationship was reversed; the denser part had the longer mean free path.

No attempts have yet been made to determine particle size changes during sintering. X-ray measurements of grain size have indicated, however, that powder particles are composed of several grains or subgrains and that the grain size approximately doubles during sintering.

B. Surface Area Measurement

Exploratory measurements of surface area were made by two techniques, the BET method using Kr(*) and an indirect method dependent on double layer capacity. The electrochemical method is of greater interest in the determination of the surface area of impregnated plates since it has the particular advantage that the

(*) A. J. Rosenberg, J. Amer. Chem. Soc. 78, 2929 (1956).

measurements are made without drying the plate. At this stage we seek only to establish the correlation between the double layer capacity and the surface area. The BET measurements carried out are listed in Table III reproducibility was better than $\pm$ 3% in three duplicate sets of measurements. A typical value for a plaque sintered at 800° C for 30 minutes using Type 255 powder is 0. 169 m^2/g. For LN-6 sintered at 720° C for 20 minutes, a higher value of 0. 535 m^2/g was recorded which is close to that of the original powder. This would indicate that temperatures of at least 800° C are necessary to produce extensive neck growth in the carbonyl powders. Neck growth is the principal mechanism for decrease in surface area and also the increase in mechanical strength and electrical conductivity. The differences in the surface area figures follow expected trends. The plaques prepared from the higher surface area powder (255) have a higher surface area. Longer sintering times or a higher sintering temperature result in a lower surface area. More detailed discussion will be reserved until more comprehensive data have been collected.

Double layer capacity measurements were made on plaques LN 12 and LN 13. The method depends on the application of a slow square wave pulse of an amplitude ot 20 mv about a potential at which the faradaic current is zero. The charging current for the double layer capacity is integrated and displayed on an oscilloscope. The shape of the trace is indicated in Fig. 3. The double layer capacity is determined from the height of the integrated trace E_ℓ by the relation

$$\text{Capacity} = \frac{R_i C_i}{R_p} \cdot \frac{E_\ell}{\Delta E}$$

TABLE VI

Surface Area Measurements

Plaque No. LN	Powder Type	Sintering Time min	Sintering Temp. °C	BET m^2/g	Double Layer Capacity $\mu F/cm^2$
12	287	30	810	0.140	10.1
13	255	30	803	0.169	15.1
14	255	30	900	0.151	
15	287	30	900	0.127	
16	255	30	800	0.168	
17	287	30	800	0.151	

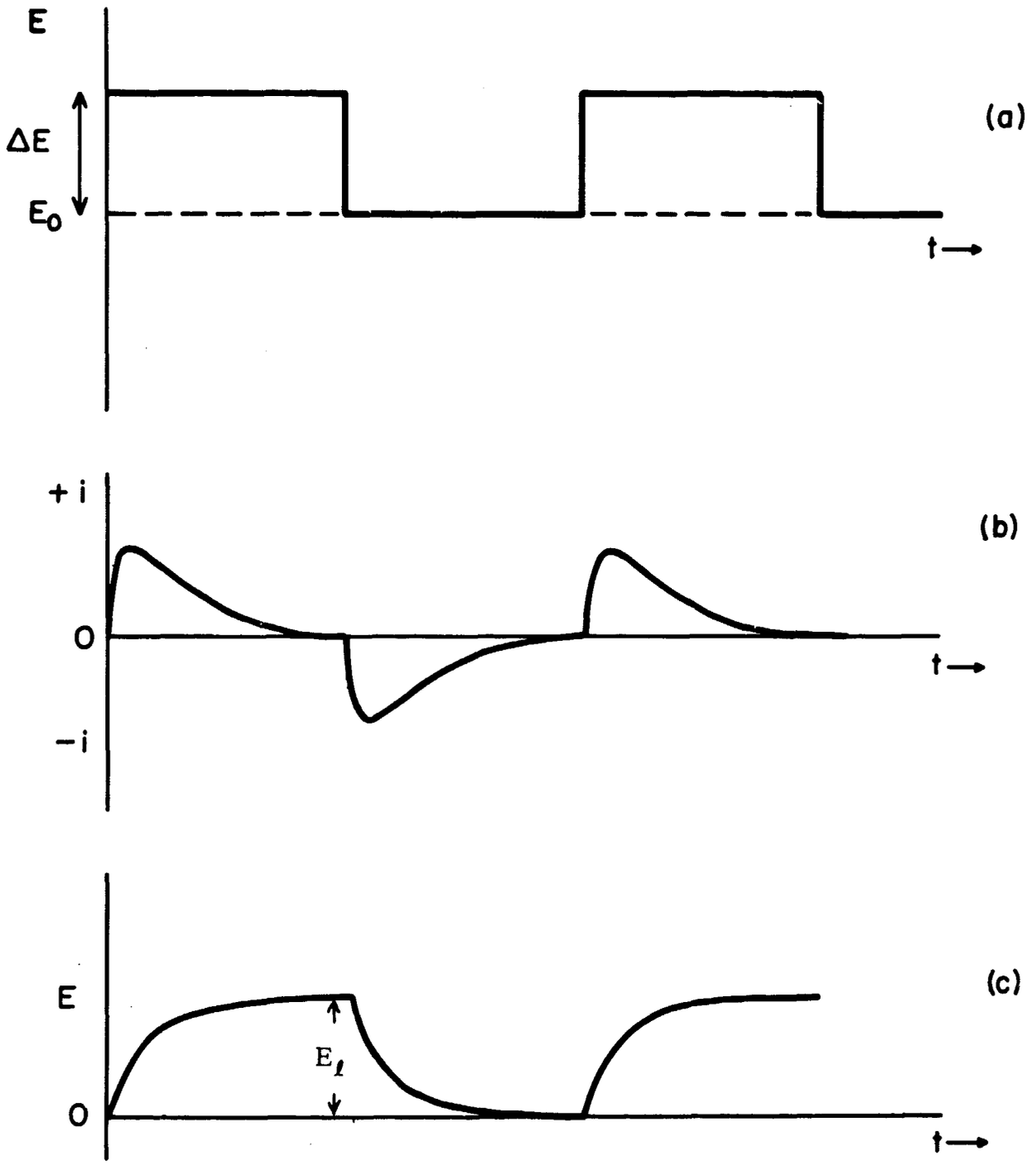

Fig. 3 Wave forms for measurement of double layer capacity:

(a) Applied potential square wave.
(b) Resulting capacity current wave.
(c) Resulting charge or capacity wave.

where R_i, C_i and R_p are constants of the integrating circuit and sampling resistor and ΔE is the height of the applied voltage signal.

The measurements were not pursued beyong the two recorded, because of difficulties with a leakage to ground in the integrator or operational amplifier. This markedly decreased the sensitivity of the method since low signal amplification at the oscilloscope was necessary to prevent the signal drifting off screen. An improved circuit design in which the leakage is eliminated is under construction for future measurements.

As indicated in Table III the two figures obtained do not yet show close correspondence to the BET figures expressed as cm^2 per square centimeter of the electrode surface. This method of expressing the surface area based on the dimensions of the sample avoids possible anomalies in the m^2/g figure due to differences in the thickness and porosity of the sample. However, the relative accuracy is less than the m^2/g figure because the electrode surface area cannot be determined as accurately as the weight. It also gives an indication of the surface roughness of the particles in the plaque, a factor that is important in determining the extent of corrosion during impregnation and the efficiency of utilization of the active material. The anomalous values for LN-14 and LN 15 of a higher surface area for the high temperature sintering cannot be explained at this stage. Future measurements will be examined closely to see if this behavior is reproduced.

C. Mercury Porosimetry

A Micromeritics mercury penetration porosimeter was used for the determination of the pore size distribution on plaque LN-4. The results are displayed in Fig. 4. A sharp pore size distribution was observed with a mean value of 7.6 μ. There was no measurable porosity below 3 μ. The mean pore size of $\sim$ 8 μ corresponds to a pressure of 20 psia, slightly above atmospheric pressure, and the transition to the second (0-1000 psia) pressure gauge of the Micromeritics 30,000 psi instrument, making measurements in the 20-30 psia range difficult.

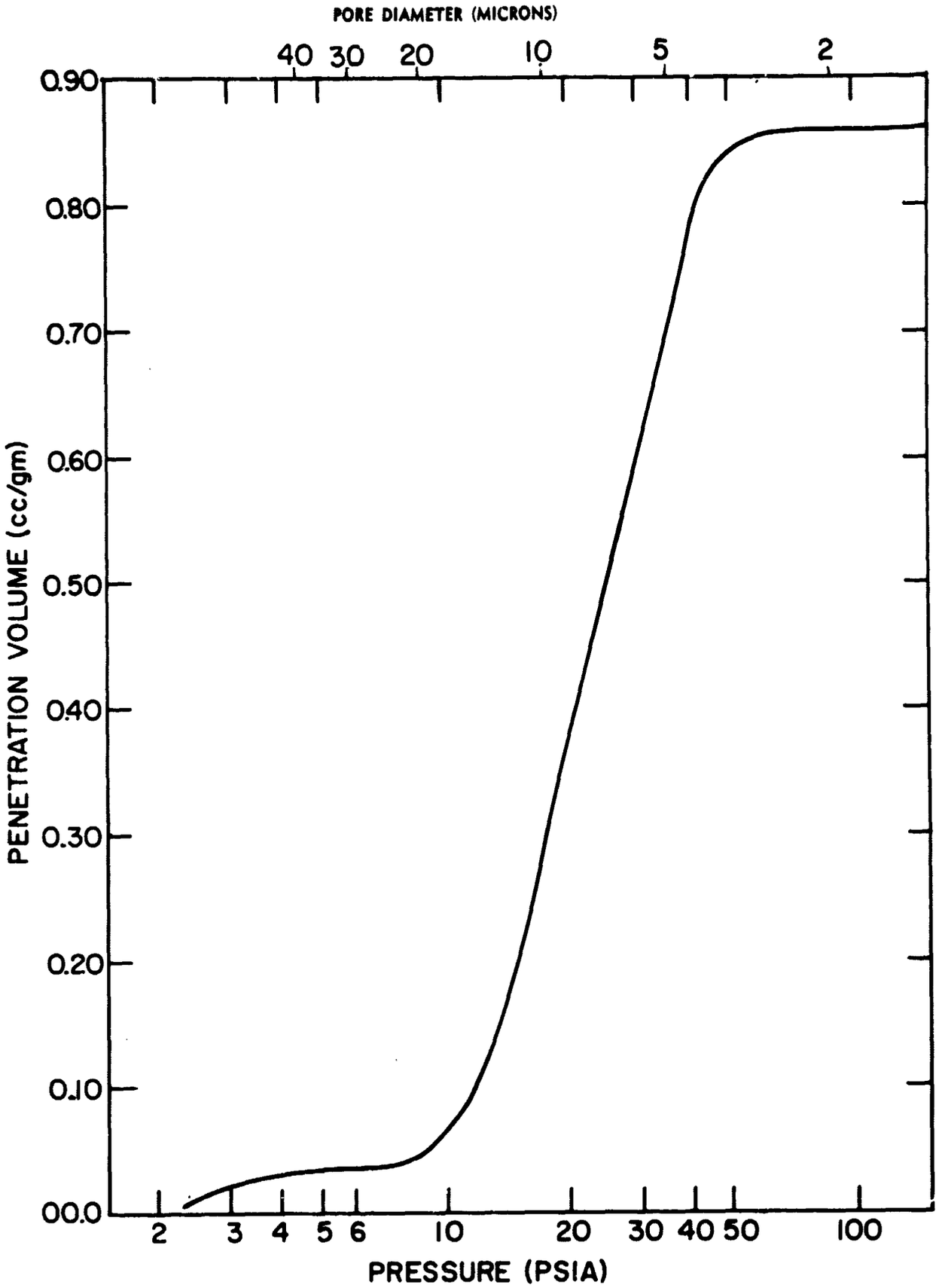

Fig. 4 Pore size distribution of LN-4 determined by mercury porosimetry.

A substitution of a 0-200 psia gauge will be made for future measurements in order to obtain more points close to the knee of the pore size distribution curve.

D. Electrical Resistivity

Resistivity was measured for plaques LN 12 through LN 17 by a four-electrode method, these results are presented in Table IV. Current carrying electrodes were attached to the full length of opposite edges of a plaque approximately 5 cm x 2 cm. The resistivity was determined by measuring the potential difference between two points a known distance apart on a line perpendicular to the edges in contact with the current carrying electrodes. The resistivity was then calculated knowing the current and the cross-sectional area of the plaque. This method of measurement avoids contributions from contact resistance, and it is possible to check that the current distribution is uniform in the region of the plauqe where the measurements are made.

The lowest resistivity was observed for the plaque prepared from the Type 287 powder sintered at 900°C. The 287 powder produced significantly lower resistivity in each case. Among the 255 powders, the plaque sintered at 900°C had the lowest resistivity.

E. Mechanical Strength

Like the electrical resistivity, a mechanical test is an indicator for the development of particle-to-particle bonds in the sintered structure. Unlike the measurement of electrical resistivity, a mechanical test in the bending mode, as opposed to a straight tensile test can be carried out so as virtually to eliminate the effects of a support in the center of the plaque. In bending, a 20 mil plaque containing a 10 mil screen in its center will reflect the strength of the sintered nickel outer layers, since 90% of the load is supported by stresses in these layers.

Figure 5 is a photograph of the completed bending jig. The gauge length between the lower supports is 1 inch, with the load applied at the quarter points. Four-point bending experiments are preferred to three-point tests, since the conditions at the center of

TABLE IV

Electrical Resistivity

Plaque No. LN	Powder Type	Sintering Time min	Sintering Temp. °C	Porosity %	Electrical Resist. ohm. cm x 10^4
12	287	30	810	87	2.80
13	255	30	803	86	4.47
14	255	30	900	83.5	2.70
15	287	30	900	78	1.61
16	255	30	800	87	3.75
17	287	30	800	83	2.50

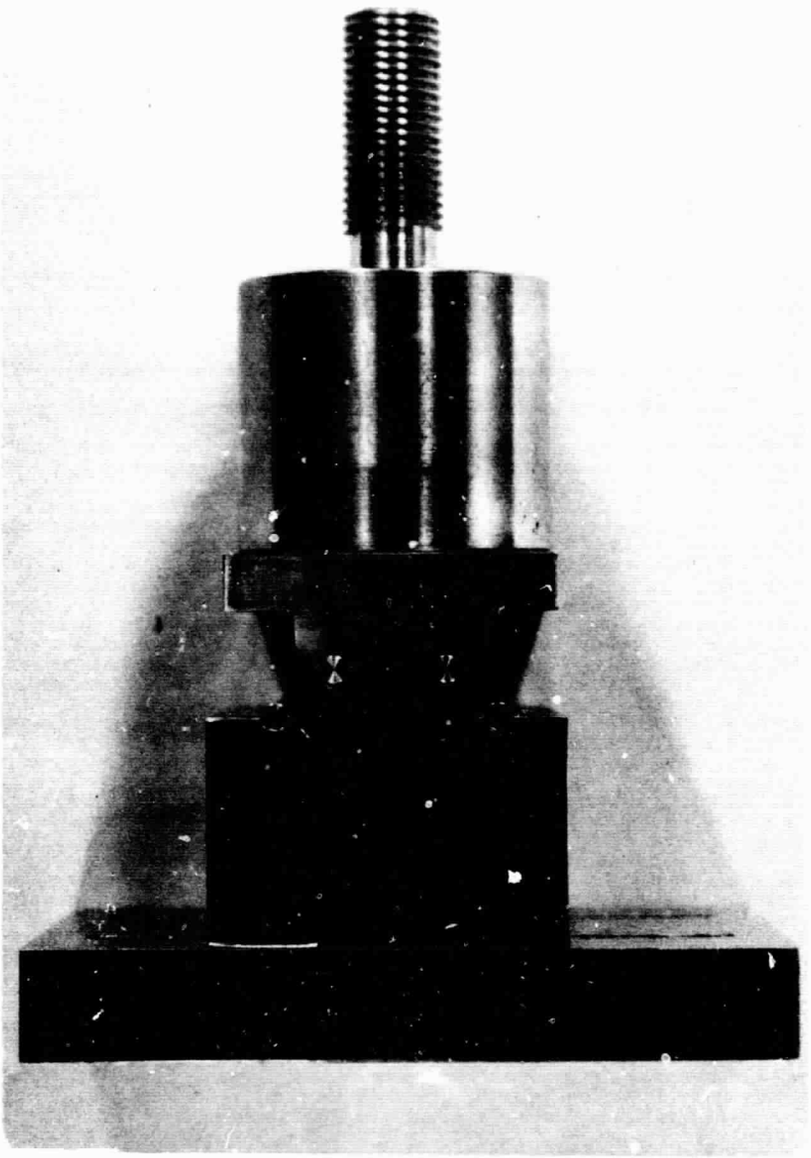

Fig. 5 Four point bend test apparatus.

the specimen length more nearly approach pure bending. The load is applied with the circular pins shown in the figure which are 1/8" in diameter.

This bending jig is used in a constant crosshead motion testing machine (Instron). The test is carried out by placing a sample, thin compared with its length, across the outer supports of the lower fixture. The fixture supporting the upper loading points is rigidly attached to the crosshead of the machine, while the lower fixture supporting the sample is placed on a flat topped compression load cell (Instron model CC load cell).

During the test, the crosshead is driven downwards, bending the sample. The displacement causes a load which is recorded as a function of time. Since the rate of deflection is known, this also gives the load as a function of the deflection. This trace (Fig. 6) shows that initially there is a linear increase of load, followed by a region of decreasing rate, and finally an abrupt drop off of the load corresponding to the failure strength of the material. This also corresponds to cracking. The point at which the curve becomes concave downwards marks the onset of plastic yielding.

The stresses and strains at any point on the linear part of this trace may be determined exactly. In the plastic portion, above the yield stress, the stress may only be calculated approximately*. The formulae for these calculations are as follows:

$$(1) \qquad \sigma = 3/4 \ \frac{PL}{bh^2}$$

where

σ = stress (psi)
P = load (lbs)
L = distance between outer supports
b = width of sample
h = thickness of sample

*Rozner, A. G., Trans. AIME 233, 1646 (1965).

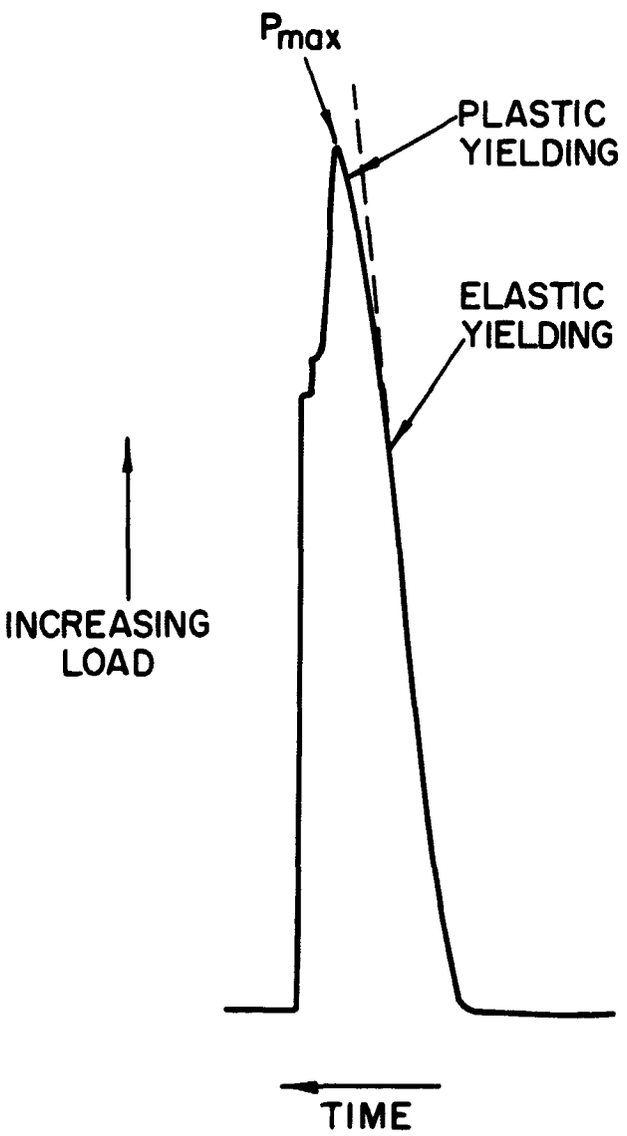

Fig. 6 Bend test LN 13.

This is the maximum stress in the outermost layers of the sample. The stress so calculated is called the modulus of rupture or simply the maximum tensile stress at failure.

The strain corresponding to any stress is obtained from Hoke's law:

$$(2) \qquad \epsilon = 3/4 \; \frac{PL}{E' \, b \, h^2}$$

where E' is the effective modulus of the porous nickel. This is related to the Young's modulus (E) by

$$(3) \qquad E' = (1 - \text{fraction porosity}) \, E.$$

Results to date have been limited to an evaluation of the method. Detailed figures for the maximum stress will be presented in the future.

IV. DISCUSSION

At this preliminary stage with a limited amount of data, it is too early to attempt a quantitative analysis of the effect of the powder characteristics and the sintering conditions on the physical nature of the plaque.

Among the data available, the trends are as expected. The plaques with the lowest porosity have the lowest surface area and resistance, and for each of the two powders the lowest porosity is obtained with longer sintering times or lower sintering temperatures. In terms of surface area and porosity the plaques prepared from different powders reflect the physical properties of the powders.

The only anomaly is the difference between the mean free path determined metallographically and the mean pore diameter derived from a mercury porosimetry. The mean pore diameter of 7.8 μ is typical of figures reported in the literature; however, a mean free path of approximately 20 μ was obtained in eight different metallographic determinations. Several alternative explanations are possible. First, the value assumed for the contact angle of mercury (130°) could be in error; however, it is unlikely that it could account for the factor of two difference between the two methods. It is also possible that the structure of the highly porous nickel plaque deviates to too great an extent from the model of the cylindrical pore on which the porosimetry calculation is based. Lastly, the metallography is open to question in that the experimental technique of impregnation with an epoxy resin under vacuum might result in changes in pore structure. It is also possible that the pore size distribution in a section of the electrode perpendicular to the surface is different from that in the surface itself. These alternatives will be examined in more detail when further porosimetry data have been collected.